



**HAL**  
open science

## Evolution of a novel left-right asymmetry involving tissue remodelling and MyoID

Bénédicte M Lefèvre, Marine Delvigne, Josué Vidal, Virginie Courtier-Orgogozo, Michael Lang

► **To cite this version:**

Bénédicte M Lefèvre, Marine Delvigne, Josué Vidal, Virginie Courtier-Orgogozo, Michael Lang. Evolution of a novel left-right asymmetry involving tissue remodelling and MyoID. 2022. hal-03868427

**HAL Id: hal-03868427**

**<https://hal.science/hal-03868427v1>**

Preprint submitted on 23 Nov 2022

**HAL** is a multi-disciplinary open access archive for the deposit and dissemination of scientific research documents, whether they are published or not. The documents may come from teaching and research institutions in France or abroad, or from public or private research centers.

L'archive ouverte pluridisciplinaire **HAL**, est destinée au dépôt et à la diffusion de documents scientifiques de niveau recherche, publiés ou non, émanant des établissements d'enseignement et de recherche français ou étrangers, des laboratoires publics ou privés.

# 1 Evolution of a novel left-right asymmetry 2 involving tissue remodelling and MyoID.

3 Bénédicte M. Lefèvre<sup>1,2</sup>, Marine Delvigne<sup>1</sup>, Josué Vidal<sup>1</sup>, Virginie Courtier-  
4 Orgogozo<sup>1\*¶</sup>, and Michael Lang<sup>1,3\*¶</sup>

5 <sup>1</sup>Université Paris Cité, CNRS, Institut Jacques Monod, F-75013 Paris, France.

6 <sup>2</sup>current address: Team “Stem Cells and Tissue Homeostasis”, Institut Curie, CNRS, UMR3215,  
7 INSERM U934, PSL Research University, 26 rue d’Ulm, 75248 Paris Cedex 05

8 <sup>3</sup>current address: Laboratoire Évolution, Génomes, Comportement et Écologie, CNRS, IRD,  
9 Université Paris-Saclay – Institut Diversité, Ecologie et Evolution du Vivant (IDEEV), 91190 Gif-  
10 sur-Yvette, France

11 <sup>¶</sup>co-last authors.

12 \*co-corresponding authors:

13 Michael Lang, **Email:** [michael.lang@universite-paris-saclay.fr](mailto:michael.lang@universite-paris-saclay.fr), Virginie Courtier-Orgogozo,

14 **Email:** [virginie.courtier@normalesup.org](mailto:virginie.courtier@normalesup.org)

## 15 Abstract

16 Left-right asymmetries recurrently evolve in animals but the underlying  
17 developmental mechanisms are unknown. In most *Drosophila* species, the male  
18 genitalia is symmetric and undergoes a clockwise 360° rotation during  
19 development. In *D. melanogaster*, this tissue remodeling process is directed by  
20 class I myosins: in MyoID mutants the rotation is reversed and the genitalia  
21 remains symmetric. Males of *Drosophila pachea* have evolved unique left-right  
22 asymmetric genital organs and a characteristic right-sided copulation posture in  
23 the past 3-6 million years. To test if these asymmetries in morphology and  
24 behavior evolved via the recruitment of pre-existing directional cues controlled by  
25 MyoID, we used CRISPR to knockout MyoID in *D. pachea*. Strikingly, mutant  
26 males undergo a reverse genitalia rotation and develop mirror-image asymmetric  
27 genitalia, indicating that MyoID controls both the direction of genitalia rotation  
28 direction and morphological asymmetry. Although genital asymmetry is reversed,  
29 MyoID mutants still adopt a wild-type right-sided copulation posture. Our results  
30 show that MyoID and its asymmetry guidance role were recruited for the  
31 evolution of a novel left-right asymmetry in *D. pachea* and that lateralized  
32 copulation behavior is determined by other mechanisms. The evolution of a new  
33 left-right organ size asymmetry in *D. pachea* involved recruitment of existing  
34 directional cues.

## 35 **Introduction**

36 While the outer bodyparts of most bilaterian animals are left-right symmetric,  
37 some organs display left-right asymmetries in position, shape or size (Hamada  
38 and Tam, 2020). The generation of asymmetric organs during development starts  
39 with an initial symmetry-breaking step, which can involve several mechanisms:  
40 motile cilia and directional fluid flow, orientation of the cell division plane and  
41 distribution of molecules within cells (Hamada and Tam, 2020). How over the  
42 course of evolution initially symmetrical organs become asymmetric remains  
43 elusive. Males of the fruitfly *Drosophila pachea* have an asymmetric phallus with  
44 a right-sided opening for sperm release (gonopore) and a pair of asymmetric  
45 external genital lobes, with the left lobe being 1.5 times longer than the right lobe  
46 (Fig 1 A,B) (Acurio et al., 2019; Lang and Orgogozo, 2012; Pitnick and Heed,  
47 1994). The lobes are considered an evolutionary novelty since they are not  
48 present in the three closely related sister species (Lang et al., 2014). *D. pachea*  
49 flies also mate in a right-sided posture with the male being shifted about 6-8°  
50 towards the right side of the female (Acurio et al., 2019; Lang and Orgogozo,  
51 2012; Rhebergen et al., 2016). The lobes function as a grasping device and  
52 stabilize the copulatory complex at the onset and during copulation (Lefèvre et  
53 al., 2021; Rhebergen et al., 2016). Asymmetric male genitalia and right-sided  
54 mating behavior have probably repeatedly evolved in *D. pachea* and closely  
55 related species within the past 3-6 Ma (Acurio et al., 2019; Lang et al., 2014).  
56 Genital asymmetry has been hypothesized to evolve in response to changes in  
57 mating position (Huber, 2010). Alternatively, asymmetric genitalia may provoke  
58 lateralized mating behavior since the asymmetric parts mediate the coupling of  
59 the female and male abdomen during copulation. Overall, the reciprocal effects  
60 of behavioral changes and evolution of morphology cannot be generalized and  
61 require case-specific assessments, in particular with respect to reproduction  
62 (Huber, 2010).

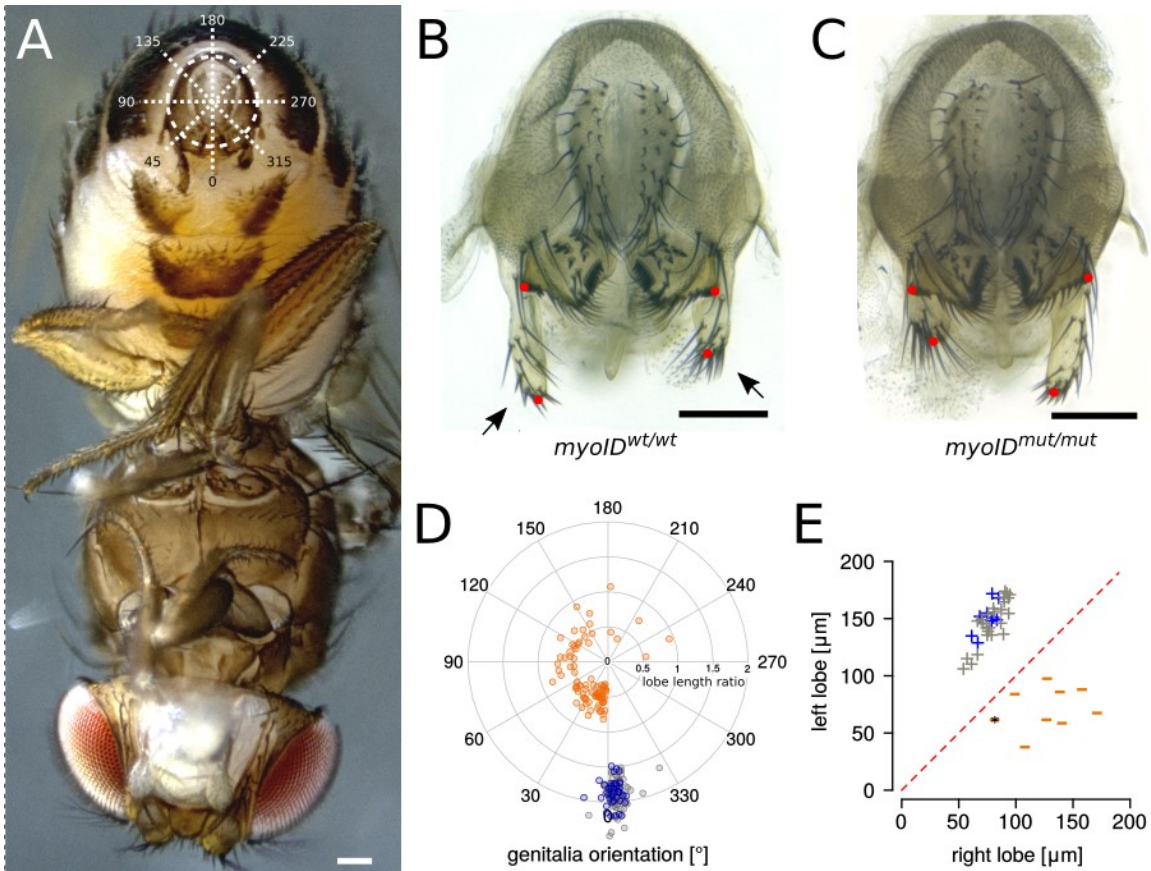
63 During development, the male genitalia of a wide range of shizophoran flies  
64 undergo a 360° clockwise rotation (Feuerborn, 1922; Suzanne et al., 2010). In *D.*  
65 *melanogaster*, the direction of this rotation is driven by the myosin MyoID,

66 encoded by the gene *myo31DF* (Spéder et al., 2006), for simplicity here referred  
67 to as *myoID*. Loss of function of *myoID* in *D. melanogaster* leads to a counter-  
68 clockwise 360° genitalia rotation direction, due to the function of another counter-  
69 acting myosin, MyoIC (Petzoldt et al., 2012; Spéder et al., 2006; Suzanne et al.,  
70 2010). MyoID also controls the chirality of other organs, such as the gut and  
71 testes (Benitez et al., 2010; González-Morales et al., 2015; Hatori et al., 2014;  
72 Hozumi et al., 2006; Okumura et al., 2015; Spéder et al., 2006; Taniguchi et al.,  
73 2011, 2007). Furthermore, MyoID appears to be a conserved key factor among  
74 different mechanisms to establish left-right asymmetry in vertebrates and  
75 invertebrates (Juan et al., 2018; Tingler et al., 2018), through interaction with  
76 adherens junctions (Petzoldt et al., 2012; Taniguchi et al., 2011), the actin  
77 cytoskeleton (Chougule et al., 2020; Lebreton et al., 2018; Petzoldt et al., 2012),  
78 planar cell polarity pathway members (González-Morales et al., 2015; Juan et al.,  
79 2018) and Jun kinase pathway regulated apoptosis (Benitez et al., 2010; Macias  
80 et al., 2004; Rousset et al., 2010; Taniguchi et al., 2007). Ectopically expressed,  
81 MyoID and MyoIC are sufficient to induce *de novo* directional twisting at the cell,  
82 organ, or body scale in *D. melanogaster* (Lebreton et al., 2018). However, the  
83 evolutionary transitions to *novel* left-right size asymmetries remain to be  
84 uncovered at the molecular, cellular and tissue scale.

## 85 **Results & Discussion**

86 We wondered if MyoID is involved in the establishment of left-right asymmetry in  
87 *D. pachea* male genitalia (Figure 1 A,B). To test this, we generated a mutation in  
88 the coding sequence of the *D. pachea myoID* using CRISPR/Cas9 mediated  
89 gene editing (Bassett et al., 2013; Jinek et al., 2012) (*myoID<sup>mut</sup>* allele, Figure 1  
90 supplement 1). The induced mutation caused a frameshift in the seventh coding  
91 exon, leading to a premature stop codon (Materials and Methods). In  
92 homozygous *myoID<sup>mut/mut</sup>* males, the length ratio of left and right genital lobes was  
93 reversed with a longer right lobe and a shorter left lobe in most (81/82) dissected  
94 individuals (Source datafile 1, Figure 1C). Furthermore, the phallus asymmetry  
95 was reversed in *myoID<sup>mut/mut</sup>* males with the gonopore located at the left tip of the  
96 phallus (29/29 dissected genitalia), compared to heterozygous *myoID<sup>wt/mut</sup>* and

97 *myoID*<sup>wt/wt</sup> males, where the gonopore was located consistently on the right side  
98 (8/8 and 13/13 dissected genitalia, respectively; Figure 1 supplement 2). The  
99 locus *myoID* is autosomal (Figure 1 supplement 1) and the mutation appears to  
100 be recessive since *myoID*<sup>wt/mut</sup> males did not have visible alterations of male  
101 genitalia morphology compared to *myoID*<sup>wt/wt</sup> males (Figure 1B). Apart from  
102 phallus and lobe morphology, homozygous mutant males revealed a genitalia  
103 rotation phenotype, with varying orientations of the male genitalia in adults, with  
104 respect to the antero-posterior midline (Figure 1 A,D). In wild-type *D. pachea*,  
105 male claspers and genital lobes are pointing towards the ventral side (Figure 1A),  
106 while *myoID*<sup>mut/mut</sup> males revealed variable orientations of genitalia, which varied  
107 among individuals between 0 and 270° (Figure 1D). This latter orientation  
108 phenotype was similar to previous observations in *D. melanogaster myoID*  
109 mutants (Spéder et al., 2006). Our data shows that MyoID is essential to  
110 determine left-right identity in *D. pachea* male genitalia, including external genital  
111 lobes and the male phallus. This function might be mediated through its role in  
112 determining the direction of male genitalia rotation. In one *myoID*<sup>mut/mut</sup> males,  
113 genital lobe asymmetry was not reversed although genitalia were mis-oriented  
114 and in one individual lobes were strongly bent. However, it was unclear if their  
115 genitalia rotated clockwise or counter-clockwise during development. These  
116 mutants may have had remnant activity and expression of the *myoID*<sup>mut</sup> allele,  
117 leading to a partial rotation in clockwise direction. Alternatively, other unidentified  
118 environmental or genetic factors may also contribute to the determination of  
119 genital asymmetry in *D. pachea* and were variable in our experiment.

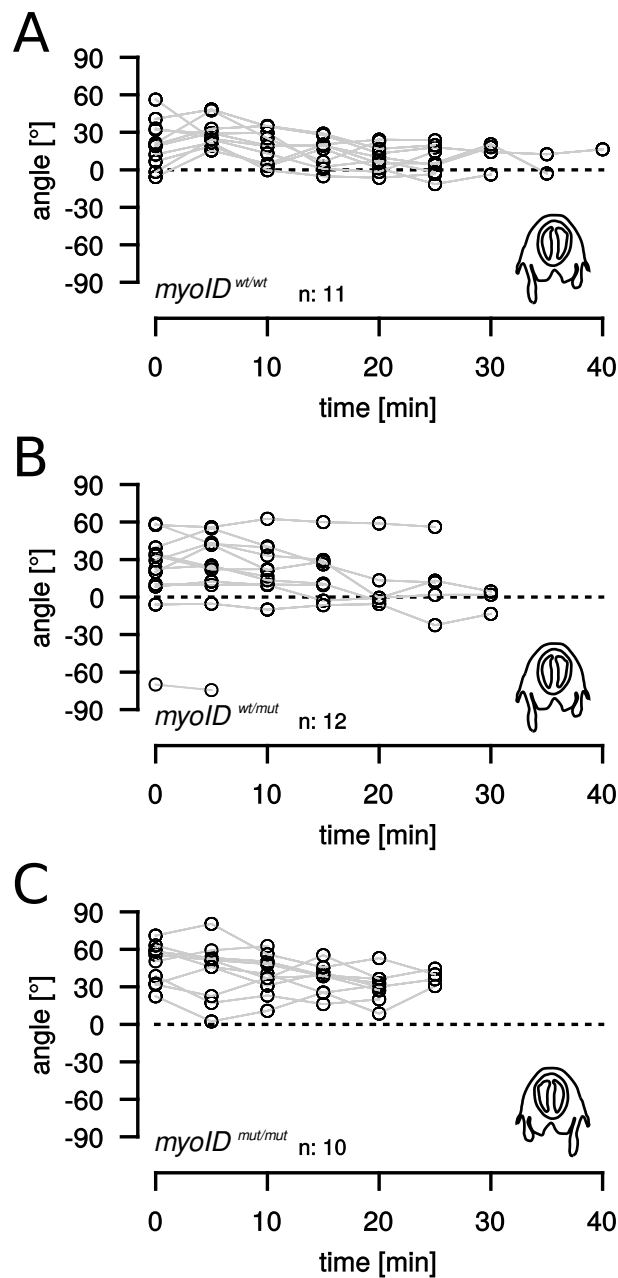


120 **Fig 1. *MyoID* mutants display reversed genital asymmetry and genitalia**  
 121 **rotation defects. (A)** Wild-type *D. pachea* male in ventral view. The orientation  
 122 of genitalia is measured as an angle between the midpoint of male genital  
 123 claspers relative to the male midline, as depicted by the dashed polar diagram.  
 124 The scale is 100  $\mu\text{m}$ . **(B)** External adult male genitalia of a wild-type male  
 125 *myoID<sup>wt/wt</sup>* with asymmetric genital lobes at the ventral side (arrows). **(C)** External  
 126 adult male genitalia of a *myoID<sup>mut/mut</sup>* mutant male with reversed genital  
 127 asymmetry. **(B-C)** Lobes are indicated by arrows and lobe length measurement  
 128 landmarks are shown as red dots. The scale is 100  $\mu\text{m}$ . **(D)** Male genitalia  
 129 orientation angles and lobe length asymmetry ratio in wild-type *myoID<sup>wt/wt</sup>* males  
 130 (blue), heterozygous *myoID<sup>wt/mut</sup>* mutant males (grey) and homozygous  
 131 *myoID<sup>mut/mut</sup>* mutant males (orange). **(E)** The direction of genital lobe asymmetry is  
 132 associated with the direction of male genitalia rotation. Left and right lobe lengths  
 133 are plotted for individual males monitored by time-lapse microscopy. Genitalia  
 134 rotation direction is indicated as +: clockwise, and as -: counter-clockwise. The  
 135 diagonal red dashed line indicates the 1:1 lobe length ratio. The star indicates an  
 136 observation with rudimentarily developed lobes in form of buds on both sides.  
 137 To monitor genitalia rotation, we inserted a DE-Cadherin::EYFP fusion construct  
 138 (DE-Cad::EYFP\_2) (Material and Methods) into the *myoID<sup>mut/mut</sup>* stock using  
 139 piggybac transposon mediated germline transformation (Horn et al.,  
 140 2003) (Source datafile 2). We examined male genitalia rotation in pupae that

141 were heterozygous for DE-Cad::EYFP to reduce potentially deleterious effects of  
142 the piggybac insert (Figure 1 supplement 3) by time-lapse microscopy (Materials  
143 and Methods). We observed that *myoID*<sup>wt/wt</sup> and *myoID*<sup>wt/mut</sup> males underwent  
144 clockwise genitalia rotation direction (movie 1, n = 9/9, 25/25, respectively), as  
145 observed in most schizophoran flies (Feuerborn, 1922; Suzanne et al.,  
146 2010) whereas in *myoID*<sup>mut/mut</sup> males, genitalia rotated counter-clockwise (movie  
147 2, n = 9/9) (Figure 1E, Source datafile 1). In 9 monitored males that had  
148 developed at least to the pharate adult stage, we were able to dissect male  
149 genitalia and to determine the orientation and the lobe length ratio of male  
150 genitalia (Figure 1E, Figure 1 supplement 2). All these *myoID*<sup>mut/mut</sup> males with  
151 counter-clockwise genitalia rotation direction had a reversed lobe length ratio  
152 with a longer right lobe and a shorter left lobe, although in one observation lobes  
153 were only rudimentarily developed and the measurements were not informative  
154 about the lobe length ratio (Figure 1E). In contrast, *myoID*<sup>wt/wt</sup> and *myoID*<sup>wt/mut</sup>  
155 males had a wild-type lobe ratio (Figure 1E). We conclude that in *D. pachea*  
156 males MyoID controls genitalia rotation direction, such as previously observed in  
157 *D. melanogaster* and that in addition, MyoID determines left-right identity of  
158 genitalia. This latter function could be mediated through direct mechanical  
159 interactions or friction forces between rotating genitalia and non-rotating outer  
160 tissue, that are expected to act in opposite direction at the left and the right side  
161 and potentially depend on of the sense of rotation.

162 We investigated if males with reversed genital asymmetry would adopt a reverted  
163 copulation posture by monitoring copulation behavior (Figure 2, Source datafile  
164 3,4, and 5) of *myoID*<sup>wt/wt</sup>, *myoID*<sup>wt/mut</sup>, or *myoID*<sup>mut/mut</sup> males with wildtype *myoID*<sup>wt/wt</sup>  
165 females. We annotated the timing of courtship and copulation (Figure 2  
166 supplement 1, Source datafile 4) and in particular we examined copulation  
167 postures (Figure 2 supplement 2, Source datafile 5). A copulation was considered  
168 to occur when the male mounted the female and achieved to settle into an  
169 invariant copulation position for at least 30 seconds. Alternatively, males were  
170 sometimes observed to mount the female, but leg and abdomen movements did  
171 not settle and eventually the male separated from the female within a few

172 minutes, which we considered to be a failed mounting attempt (106/140 total  
173 attempts, Figure 2 supplement 1). Only 26% (10/38) of the couples with  
174 *myoID<sup>mut/mut</sup>* males that mounted the female also adopted a stable copulation  
175 position, compared to 11/11 and 13/13 for *myoID<sup>wt/wt</sup>* and *myoID<sup>wt/mut</sup>* males,  
176 respectively. Genitalia orientation angles of *myoID<sup>mut/mut</sup>* males that managed to  
177 adopt a stable copulation posture were found to deviate at most by 16.7° from  
178 wild-type orientations, while it was higher in the majority of *myoID<sup>mut/mut</sup>* males  
179 (18/29) that failed to copulate (Figure 1D, Figure 2 supplement 1). Such defects  
180 in genitalia orientation were previously reported to be detrimental for copulation  
181 and efficient genitalia coupling for *D. melanogaster myoID* mutants (Inatomi et  
182 al., 2019). Regardless of the genotype and direction of genital asymmetry,  
183 *myoID<sup>wt/wt</sup>*, *myoID<sup>wt/mut</sup>* and *myoID<sup>mut/mut</sup>* males consistently adopted a right-sided  
184 average copulation posture (Figure 2). Overall, right-sided mating posture in *D.*  
185 *pachea* does not depend on the direction of male genital asymmetry. Right-sided  
186 mating is therefore female-controlled or may be a hard-wired behavior that could  
187 have possibly favored the evolution of morphological asymmetry as an instructive  
188 cue to optimize genital contacts (Huber, 2010).



189 **Fig 2. The right-sided *D. pachea* mating posture does not depend on the**  
 190 **direction of male genital asymmetry.** Mating angles ( $\alpha$ ) (S1 File) of virgin *D.*  
 191 *pachea* wild-type females *myoID*<sup>wt/wt</sup>, copulating with a male being either **(A)**  
 192 *myoID*<sup>wt/wt</sup> with the wild-type lobe length ratio, **(B)** *myoID*<sup>wt/mut</sup> heterozygous males  
 193 with wildtype lobe length ratio, **(C)** *myoID*<sup>mut/mut</sup> males with reverted lobe  
 194 asymmetry ratio. The hypothesis angle = 0 was rejected for each male genotype  
 195 (GLM fit angle  $\sim$  genotype, all  $p < 1 \times 10^{-10}$ ). Data acquisition and processing is  
 196 illustrated in Figure 2 supplements 1 and 2. Positive angle values correspond to  
 197 right-sided orientations of the male head relative to the female midline. Data  
 198 points that correspond to the same trial are connected by grey lines. The number  
 199 of trials are indicated by n, a drawing of the external male genitalia of each  
 200 genotype is shown on the right.

201 This study provides the first experimental insights into *de novo* Evolution of left-  
202 right asymmetry. It involves recruitment of a conserved left-right regulator and is  
203 associated with a pre-existing tissue remodeling process. Our study reveals  
204 functional conservation of the unconventional myosin MyoID to control clockwise  
205 genitalia rotation in developing *D. pachea* male genitalia. In addition, the same  
206 protein got co-opted during evolution of *D. pachea* to contribute to determination  
207 of the direction of a novel male genital asymmetry. The latter function may be  
208 mediated through the genitalia rotation process itself since rotation direction and  
209 genital asymmetry direction are perfectly associated in our live-imaging trials.  
210 Male genital asymmetry does not determine the lateralized mating posture  
211 observed in *D. pachea* since wildtype and mutant males with reversed genital  
212 asymmetry consistently mate in a right-sided copulation posture. Right-sided  
213 mating is therefore female-controlled or may be a hard-wired behavior to  
214 optimize the complex of female and male organs during copulation.

## 215 **Materials and Methods**

### 216 **Generation of MyoID mutants**

217 The *D. pachea myoID* ortholog was identified by sequence comparisons of *D.*  
218 *melanogaster myoID* cDNA sequence NM\_001201855.2 and the *D. pachea*  
219 genome assembly JABVZX000000000 (Suvorov et al., 2021) (Figure 1  
220 supplement 1). CRISPR targets were searched manually and single guide RNA  
221 synthesis was performed *in vitro* according to (Bassett et al., 2013) (Table 1).

222 **Table 1. Oligonucleotides for PCR and preparation of CRISPR sgRNA.** Tan °C: annealing  
 223 temperatures used in our experiments. \*: touch-down annealing temperature

oligo-nucleotide	sequence	Tan °C	reference
pacMyoID-retro	CCTAATATGATACACCGAACTAT	50	this study
pacMyoID-debut	GAGCAAAACAAAACGAGAAACAT	60	this study
pacMyoID-stop	CGCTCAGCAGCTATCAGCTCTAA	60	this study
2F_Dpac_m31DF	TCGCCAGGACTTCCGCATTA	60	this study
4F_Dpac_m31DF	CCAATTCGAGGACAACAG	60	this study
1R_Dpac_m31DF	GCCGATTACCGAGTTGAATCT	60	this study
Dpa2Rbis3	CGCAGCAGGAACTTGTGTA	60	this study
Dpa_myoIDCRISP	GAAATTAATACGACTCACTATAGGTTGAACACGCTGCTAAAGAGTTTTAGAGCTAGAAATAGC	60	this study
R_F	AAAAGCACCGACTCGGTGCCACTTTTTCAAGTTGATAACGGACTAGCCTTATTTAACTTGCAT	60	(Basset et al 2013)
CRISPR-sgR	TTCTAGCTCTAAAAC	60	
1F_Dpac_m31DF	CGCCAACCTGGACCTGCATAA	70-60*	this study
MyoID_3F-genoF1	ATTATCCAGCGGTACATGGCCGAT	62	this study
m_DECad_R1	CGGCTGGCGAAGATTCTTA	62	this study
m_DECad_F1	CCTGCAGGTCGACCACTCGAGTGTTGCATTGTGTTTTGC	62	this study
mDECad_R2	CAATGATGAAAAATGATGGCGGCTTAATTG	64	this study
mDECad_F2	GCCATCATTTTTCATCATTGCGATCATCGTATG	64	this study
m_DECad_R3	TTGGGAGCTCTCCCATACTCGAGCACATCGTCCACGGTTGTG	60	this study
act5C_F1	GGTTACGGCACTAGAGCGGCGCGCAATTCTATATTCTAAAAACACAAATGATACTTCTAAAA	60	this study
act5C_R	AAAACATACATATGACATGTGTTTTATAGTGGGTTTATTAG	65	this study
act5C_F2	TATAAACACATGTACATATGTATGTTTTGGCATAACAATGAGTAGTTG	65	this study
SV40_R	TACCGTCGACCTCGAGAGATCTGATCCAGACATGATAAGATACATTGATGAGTTGGACAAACCA	64	this study
InvPCR_F1	CAACTAGAA	64	this study
InvPCR_R1	CGGCGACTGAGATGTCCTAAAT	64	this study
InvPCR_F2	GCCGTAAGTGTCACTGATTTTGAACATAA	64	this study
InvPCR_R2	CGCGCTATTTAGAAAAGAGAGCAATATTT	64	this study
	GACCGCGTGAGTCAAATGA		

224 sgRNA/Cas-9 complexes were injected using standard *Drosophila* germline  
 225 transformation procedures (see detailed protocol). The injection mix contained  
 226 0.1 µg/µL sgRNA, 2 µM NLS-Cas9 (New England Biolabs) and 1x NLS-Cas9  
 227 reaction Buffer (New England Biolabs). Emerging adults from injections were  
 228 crossed to non-injected individuals and resulting progeny was maintained for  
 229 several generations. Candidate stocks for CRISPR mutants were identified by  
 230 visual inspection of male adults that had genitalia rotation defects. Candidate  
 231 stocks were screened for *myoID* mutations by PCR and Sanger sequencing  
 232 (Source datafile 1). We identified a mutation at position 1724 downstream of the  
 233 translation start codon, which contained a 13-bp deletion and a 7-bp insertion  
 234 (Figure 1 supplement 1). The frameshift leads to a premature stop codon,  
 235 abolishing 443 native codons that encode the C-terminal part of MyoID (Figure 1  
 236 supplement 1 B,C, Source datafile 1). The identified mutation also contained a  
 237 *NcoI* restriction site (Figure 1 supplement 1 B), not present in the wild-type allele.  
 238 We took advantage of this restriction site to determine the genotype of *D. pachea*  
 239 individuals (Figure supplement 1 D, Source datafile 1). Prior to genotyping,  
 240 genitalia of male adults or pupae were dissected and imaged (Figure 1  
 241 supplement 2, Source datafile 1).

242

### 243 **Generation act5C::DE-Cad-EYFP\_2 flies**

244 We generated a membrane specific EYFP cellular marker pB-act5C::DE-Cad-  
245 EYFP that contains a partial *D. melanogaster* DE-Cadherin (*shg*) and EYFP  
246 coding sequences (Source datafile 1). The assembled gene construct includes  
247 the *D. melanogaster shg* 5'UTR and two initial cadherin repeats, the DE-cadherin  
248 trans-membrane domain and a part of the cytoplasmic domain without the  $\beta$ -  
249 Catenin binding domain. The gene construct was inserted into the vector  
250 backbone of pBAC-ECFP-15xQUAS\_TATA-mcd8-GFP-SV40 (Addgene 104878)  
251 and the 3xP3 ECFP integration reporter was replaced by 3xP3 DsRed (Matz et  
252 al., 1999). transgenic flies were produced by germline transformation as  
253 described above. Identification of act5C::DE-Cad-EYFP\_2 transgenic flies was  
254 achieved by evaluation of eye fluorescence driven by the 3xP3 DsRed integration  
255 reporter. The insertion site was mapped to position 14,614,126 on contig  
256 tig00000094 (Source datafile 1), inside the first 31.95-kb intron of the putative *D.*  
257 *pachea wheeler18* gene homolog.

### 258 **Genitalia live imaging**

259 We followed a particular crossing scheme to analyze genitalia rotation of varying  
260 *myoID* genotypes in a heterozygous act5C::DE-Cad-EYFP\_2 background (Figure  
261 1 supplement 3). Time-lapse microscopy of developing genitalia was performed  
262 at 20 – 25 h after the puparium had formed on a DMI8 inverted microscope  
263 (Leica), equipped with a spinning-disc head CSU-W1 (Yokogawa Corporation of  
264 America) and controlled by MetaMorph software (Molecular Devices). Imaging up  
265 to 20 samples in parallel was carried out at 200 fold magnification for 15 -24 h, by  
266 acquisition of individual z-stacks every 30 min (Source datafile 1 File).

### 267 **Evaluation of mating behavior**

268 We performed video-recording of virgin but sexually mature *D. pachea*  
269 individuals (Figure 2 supplements 1 and 2, Source datafiles 3 and 4), also  
270 described in (Acurio et al., 2019) and (Lefèvre et al., 2021). Mating position  
271 analysis (Figure 2 supplement 2, Source datafile 5) was carried out as described  
272 in (Acurio et al., 2019).

## 273 **Data availability**

274 Data supporting this article is available as Source datafiles and raw data has  
275 been deposited at the DRYAD database (doi:10.5061/dryad.bzkh189bd), except  
276 for DNA sequence data of the *D. pachea myoID* coding sequence, which was  
277 deposited at NCBI (accession number OM240650).

## 278 **Acknowledgments**

279 We thank Stéphane Prigent for preparation of *Drosophila* genitalia. We  
280 acknowledge the ImagoSeine core facility of the Institut Jacques Monod, member  
281 of IBSA and France-BioImaging (ANR-10-INBS-04) infrastructures for assistance  
282 in microscopy. We are grateful to Nicolas Gompel for initial help with *Drosophila*  
283 germline transfection.

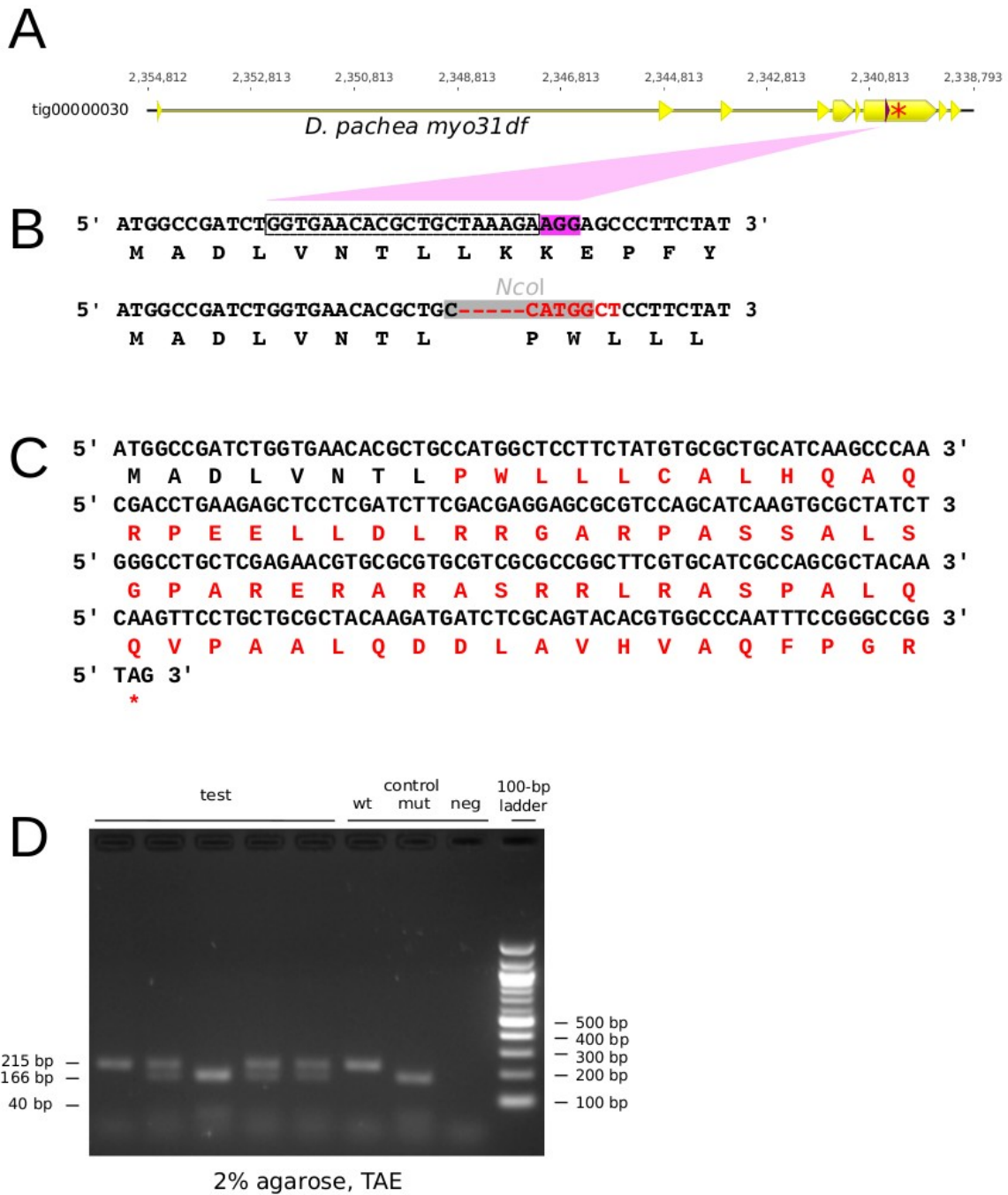
## 284 **References**

- 285 Acurio A, Rhebergen FT, Paulus SE, Courtier-Orgogozo V, Lang M. 2019. Repeated evolution of  
286 asymmetric genitalia and right-sided mating behavior in the *Drosophila* nanoptera species  
287 group. *BMC Evol Biol* **19**:109. doi:10.1186/s12862-019-1434-z
- 288 Bassett AR, Tibbit C, Ponting CP, Liu J-L. 2013. Highly Efficient Targeted Mutagenesis of  
289 *Drosophila* with the CRISPR/Cas9 System. *Cell Rep* **4**:220–228.  
290 doi:10.1016/j.celrep.2013.06.020
- 291 Benitez S, Sosa C, Tomasini N, Macias A. 2010. Both JNK and apoptosis pathways regulate  
292 growth and terminalia rotation during *Drosophila* genital disc development. *Int J Dev Biol*  
293 **54**:643–653.
- 294 Chougule A, Lapraz F, Földi I, Cerezo D, Mihály J, Noselli S. 2020. The *Drosophila* actin  
295 nucleator DAAM is essential for left-right asymmetry. *PLOS Genet* **16**:e1008758.
- 296 Feuerborn HJ. 1922. Das Hypopygium 'inversum' und 'circumversum' der Dipteren. *Zool Anz*  
297 **55**:89–213.
- 298 González-Morales N, Géminard C, Lebreton G, Cerezo D, Coutelis J-B, Noselli S. 2015. The  
299 Atypical Cadherin Dachshous Controls Left-Right Asymmetry in *Drosophila*. *Dev Cell* **33**:675–  
300 689. doi:10.1016/j.devcel.2015.04.026
- 301 Hamada H, Tam P. 2020. Diversity of left-right symmetry breaking strategy in animals.  
302 *F1000Research* **9**:F1000 Faculty Rev-123. doi:10.12688/f1000research.21670.1
- 303 Hatori R, Ando T, Sasamura T, Nakazawa N, Nakamura M, Taniguchi K, Hozumi S, Kikuta J, Ishii  
304 M, Matsuno K. 2014. Left–right asymmetry is formed in individual cells by intrinsic cell  
305 chirality. *Mech Dev* **133**:146–162. doi:https://doi.org/10.1016/j.mod.2014.04.002

- 306 Horn C, Offen N, Nystedt S, Häcker U, Wimmer EA. 2003. &lt;em>piggyBac&/em>-Based  
307 Insertional Mutagenesis and Enhancer Detection as a Tool for Functional Insect Genomics.  
308 *Genetics* **163**:647 LP – 661.
- 309 Hozumi S, Maeda R, Taniguchi K, Kanai M, Shirakabe S, Sasamura T, Spéder P, Noselli S, Aigaki  
310 T, Murakami R, Matsuno K. 2006. An unconventional myosin in *Drosophila* reverses the  
311 default handedness in visceral organs. *Nature* **440**:798–802. doi:10.1038/nature04625
- 312 Huber BA. 2010. Mating positions and the evolution of asymmetric insect genitalia. *Genetica*  
313 **138**:19–25.
- 314 Inatomi M, Shin D, Lai Y-T, Matsuno K. 2019. Proper direction of male genitalia is prerequisite for  
315 copulation in *Drosophila*, implying cooperative evolution between genitalia rotation and  
316 mating behavior. *Sci Rep* **9**:210. doi:10.1038/s41598-018-36301-7
- 317 Jinek M, Chylinski K, Fonfara I, Hauer M, Doudna JA, Charpentier E. 2012. A Programmable  
318 Dual-RNA–Guided DNA Endonuclease in Adaptive Bacterial Immunity. *Science (80- )*  
319 **337**:816–821. doi:10.1126/science.1225829
- 320 Juan T, Géminard C, Coutelis J-B, Cerezo D, Polès S, Noselli S, Fürthauer M. 2018. Myosin1D is  
321 an evolutionarily conserved regulator of animal left–right asymmetry. *Nat Commun* **9**:1942.  
322 doi:10.1038/s41467-018-04284-8
- 323 Lang M, Orgogozo V. 2012. Distinct copulation positions in *Drosophila* *pachea* males with  
324 symmetric or asymmetric: External genitalia. *Contrib to Zool* **81**:87–94.
- 325 Lang M, Polihronakis Richmond M, Acurio AE, Markow TA, Orgogozo V. 2014. Radiation of the  
326 *Drosophila* *nannoptera* species group in Mexico. *J Evol Biol* **27**:575–584.  
327 doi:10.1111/jeb.12325
- 328 Lebreton G, Géminard C, Lapraz F, Pyrpasopoulos S, Cerezo D, Spéder P, Ostap E M, Noselli  
329 S. 2018. Molecular to organismal chirality is induced by the conserved myosin 1D. *Science*  
330 (80- ) **362**:949–952. doi:10.1126/science.aat8642
- 331 Lefèvre BM, Catté D, Courtier-Orgogozo V, Lang M. 2021. Male genital lobe morphology affects  
332 the chance to copulate in *Drosophila* *pachea*. *BMC Ecol Evol* **21**:23. doi:10.1186/s12862-  
333 021-01759-z
- 334 Macias A, Romero NM, Martin F, Suarez L, Rosa AL, Morata G. 2004. PVF1/PVR signaling and  
335 apoptosis promotes the rotation and dorsal closure of the *Drosophila* male terminalia. *Int J*  
336 *Dev Biol* **48**:1087–1094.
- 337 Matz M V, Fradkov AF, Labas YA, Savitsky AP, Zaraisky AG, Markelov ML, Lukyanov SA. 1999.  
338 Fluorescent proteins from nonbioluminescent Anthozoa species. *Nat Biotechnol* **17**:969–  
339 973. doi:10.1038/13657
- 340 Okumura T, Sasamura T, Inatomi M, Hozumi S, Nakamura M, Hatori R, Taniguchi K, Nakazawa  
341 N, Suzuki E, Maeda R, Yamakawa T, Matsuno K. 2015. Class I Myosins Have Overlapping  
342 and Specialized Functions in Left-Right Asymmetric Development in *Drosophila*. *Genetics*  
343 **199**:1183–1199. doi:10.1534/genetics.115.174698
- 344 Petzoldt AG, Coutelis J-B, Géminard C, Spéder P, Suzanne M, Cerezo D, Noselli S. 2012. DE-  
345 Cadherin regulates unconventional Myosin ID and Myosin IC in *Drosophila* left-right  
346 asymmetry establishment. *Development* **139**:1874–1884. doi:10.1242/dev.047589

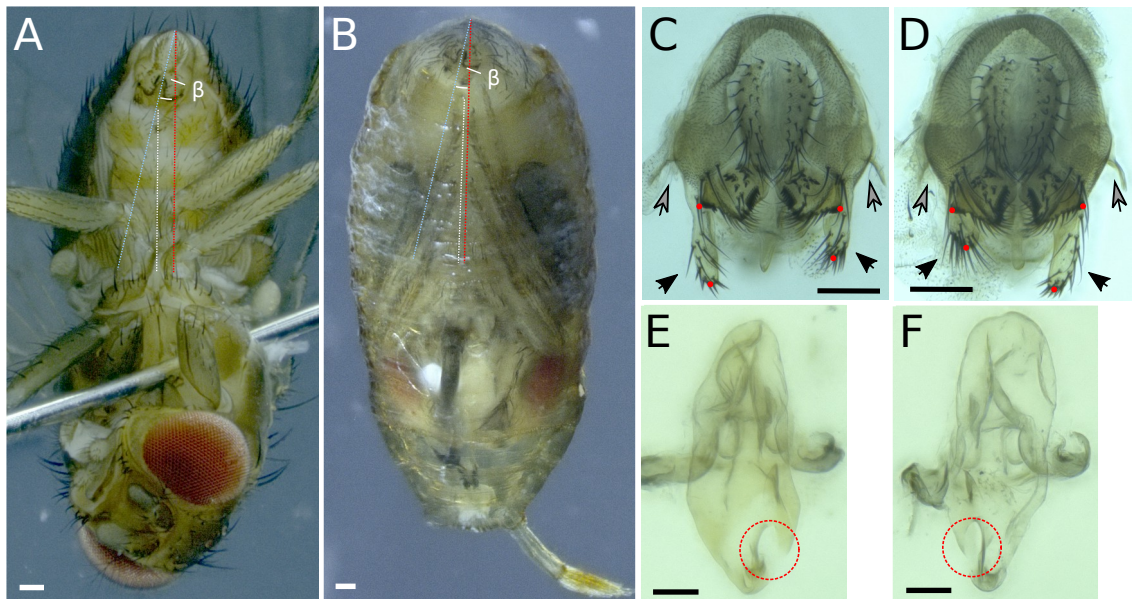
- 347 Pitnick S, Heed W. 1994. New Species of Cactus-Breeding *Drosophila* (Diptera: Drosophilidae) in  
348 the Nannoptera Species Group. *Ann Entomol Soc Am* **87**:307–310.
- 349 Rhebergen FT, Courtier-Orgogozo V, Dumont J, Schilthuizen M, Lang M. 2016. *Drosophila*  
350 *pachea* asymmetric lobes are part of a grasping device and stabilize one-sided mating.  
351 *BMC Evol Biol* **16**:176. doi:10.1186/s12862-016-0747-4
- 352 Rousset R, Bono-Lauriol S, Gettings M, Suzanne M, Spéder P, Noselli S. 2010. The *Drosophila*  
353 serine protease homologue Scarface regulates JNK signalling in a negative-feedback loop  
354 during epithelial morphogenesis. *Development* **137**:2177–2186. doi:10.1242/dev.050781
- 355 Spéder P, Ádám G, Noselli S. 2006. Type ID unconventional myosin controls left–right asymmetry  
356 in *Drosophila*. *Nature* **440**:803–807. doi:10.1038/nature04623
- 357 Suvorov A, Kim BY, Wang J, Armstrong EE, Peede D, Agostino ERR, Price DK,  
358 Wadell P, Lang M, Courtier-Orgogozo V, David JR, Petrov D, Matute DR, Schrider DR,  
359 Comeault AA. 2021. Widespread introgression across a phylogeny of 155 *Drosophila*  
360 genomes. *Curr Biol* **32**:111–123. doi:10.1101/2020.12.14.422758
- 361 Suzanne M, Petzoldt AG, Spéder P, Coutelis J-B, Steller H, Noselli S. 2010. Coupling of  
362 Apoptosis and L/R Patterning Controls Stepwise Organ Looping. *Curr Biol* **20**:1773–1778.  
363 doi:doi: 10.1016/j.cub.2010.08.056
- 364 Taniguchi K, Hozumi S, Maeda R, Ooike M, Sasamura T, Aigaki T, Matsuno K. 2007. D-JNK  
365 signaling in visceral muscle cells controls the laterality of the *Drosophila* gut. *Dev Biol*  
366 **311**:251–263. doi:https://doi.org/10.1016/j.ydbio.2007.08.048
- 367 Taniguchi K, Maeda R, Ando T, Okumura T, Nakazawa N, Hatori R, Nakamura M, Hozumi S,  
368 Fujiwara H, Matsuno K. 2011. Chirality in Planar Cell Shape Contributes to Left-Right  
369 Asymmetric Epithelial Morphogenesis. *Science (80- )* **333**:339–341.  
370 doi:10.1126/science.1200940
- 371 Tingler M, Kurz S, Maerker M, Ott T, Fuhl F, Schweickert A, LeBlanc-Straceski JM, Noselli S,  
372 Blum M. 2018. A Conserved Role of the Unconventional Myosin 1d in Laterality  
373 Determination. *Curr Biol* **28**:810-816.e3. doi:10.1016/j.cub.2018.01.075

374 **Figure supplements**

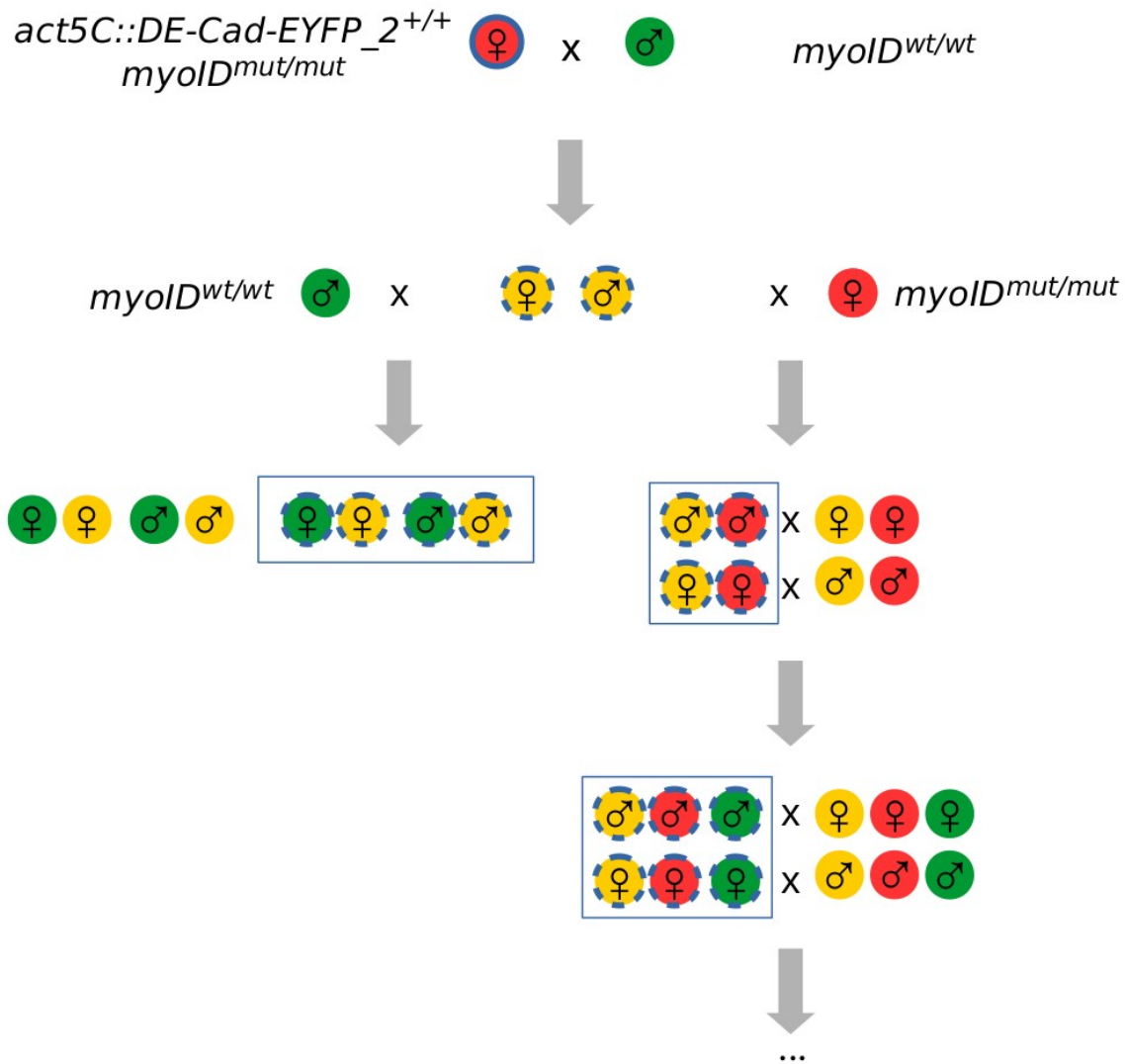


375 **Figure 1 supplement 1. Identification of the myoID mutation. (A)** Annotation  
376 of the *myoID* coding sequence (orange). Orange arrows indicate coding exons,  
377 numbers indicate the nucleotide positions relative to contig tig00000030, the  
378 violet arrow indicates the CRISPR target site and the red star indicates the  
379 location of the premature stop codon in the *myoID* mutant. **(B)** Nucleotide and  
380 amino acid sequences at the CRISPR target site. The upper line corresponds to  
381 the *D. pachea* wild-type *myoID* sequence, the lower line to the CRISPR/Cas-9  
382 induced frameshift mutation. Outlined framed positions indicate the single guide

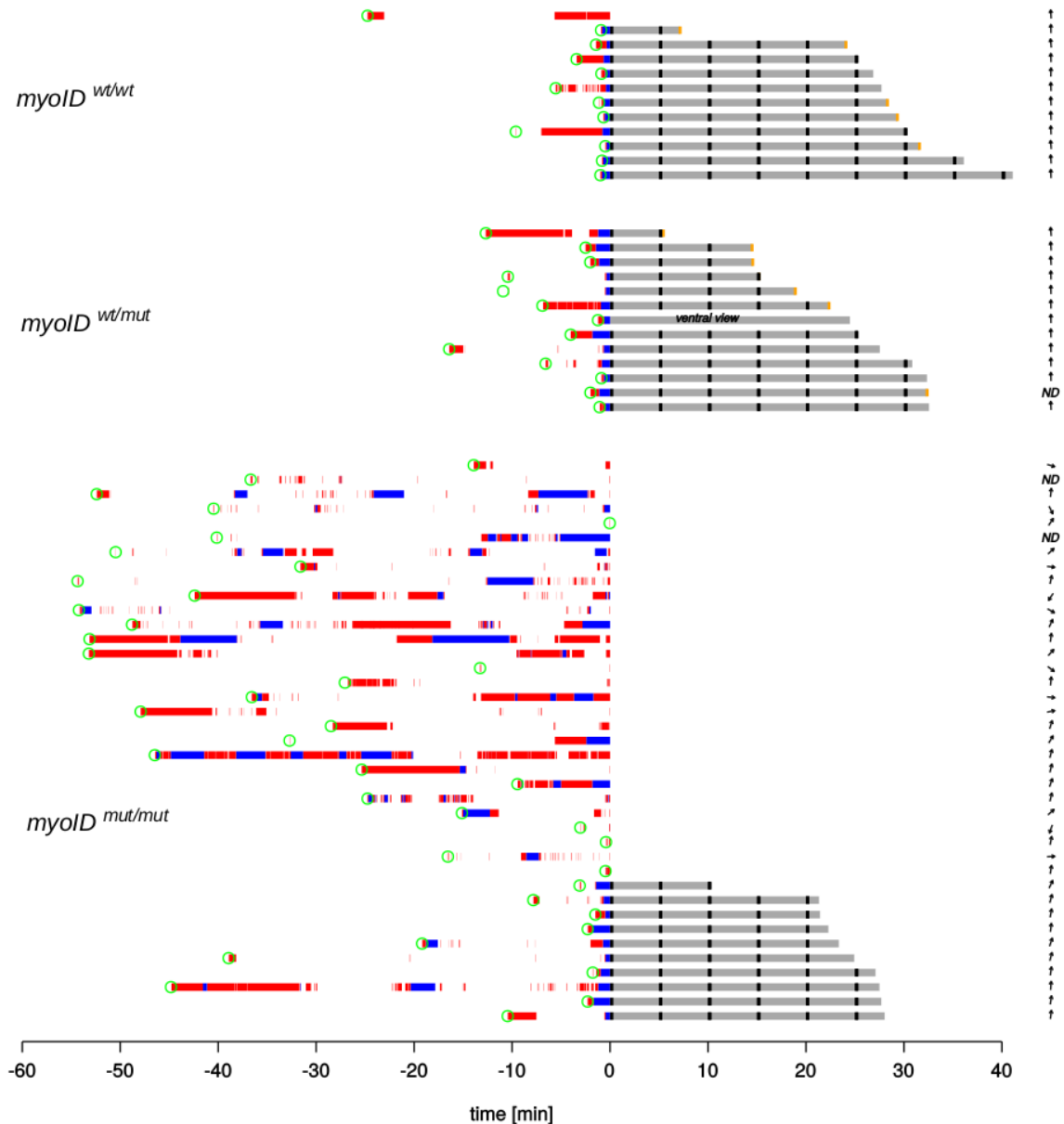
383 RNA (sgRNA) sequence to target *myoID*, dark-violet highlights the protospacer  
 384 adjacent motif (PAM). The mutated positions are in red, the *NcoI* endonuclease  
 385 motif is highlighted in grey. Single letter amino acid abbreviations are presented  
 386 beneath each codon. **(C)** The mutation causes a frameshift. Altered amino acid  
 387 sequence is indicated by red single letter amino acid abbreviations, **(D)** Gel  
 388 electrophoresis of *NcoI* digested PCR products, used to distinguish *D. pachea*  
 389 male genotypes. Test indicates lanes corresponding to genomic DNA of males  
 390 6U, 8A, 8C, 8D and 8E (Source datafile 2), used for time-lapse microscopy.  
 391 Controls indicate a *myoID*<sup>+/+</sup> male (wt), a *myoID*<sup>-/-</sup> male (mut) and a negative  
 392 control amplified from water (neg). The 100 bp ladder is presented on the right.  
 393 Relevant DNA fragment sizes are indicated at the sides of the image, the  
 394 agarose concentration and gel electrophoresis buffer is annotated below the  
 395 image.



396 **Figure 1 supplement 2. Quantification of genitalia morphology.** **(A)** Male  
 397 genitalia orientation was measured as the angle ( $\beta$ ) between the dorso-ventral  
 398 axis of male genitalia (blue dashed line) relative to the male antero-posterior  
 399 body axis (white and red dashed lines). **(B)** genitalia orientation was also  
 400 measured in male pupae where genitalia were visible. The midline was  
 401 approximated as a medial line between the ventrally located legs (white dashed  
 402 line). **(C-D)** The length of the lobes (black arrows) in wildtype genitalia **(C)**,  
 403 heterozygous *myoID*<sup>wt/mut</sup> mutants, and homozygous *myoID*<sup>mut/mut</sup> mutants **(D)** was  
 404 measured as the distance between the pointed outer edge of the surstili (upper  
 405 red points) and the medial tip of each lobe (lower red points). The lateral spine is  
 406 indicated by grey arrows. **(A-D)** The scale is 100  $\mu$ m. **(E-F)** Phallus of a  
 407 *myoID*<sup>wt/mut</sup> male **(E)** and *myoID*<sup>mut/mut</sup> male **(F)** with the gonopore (highlighted by  
 408 red dashed circles) on the right and left side, respectively. The scale is 50  $\mu$ m.

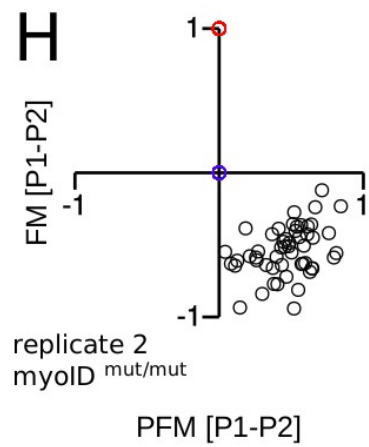
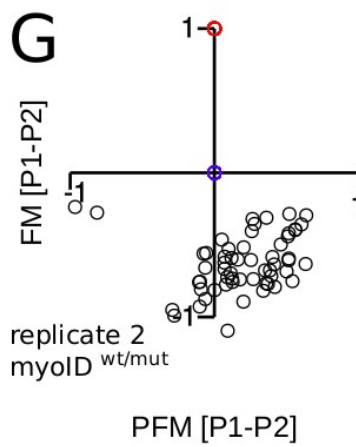
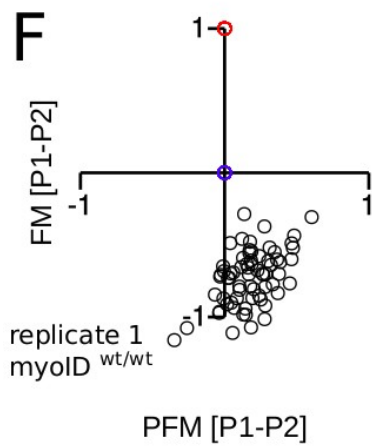
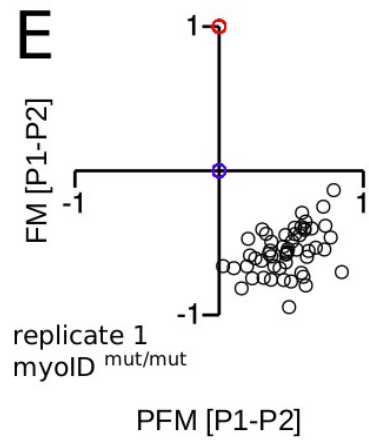
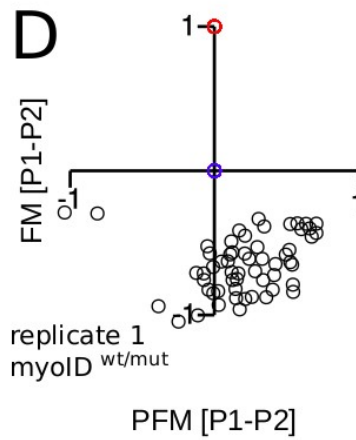
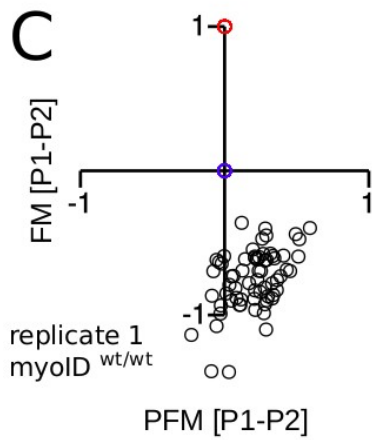
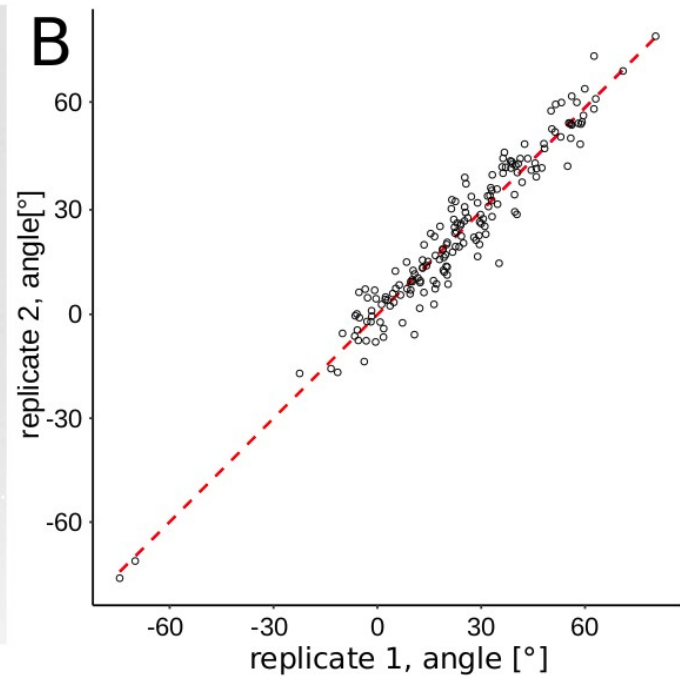
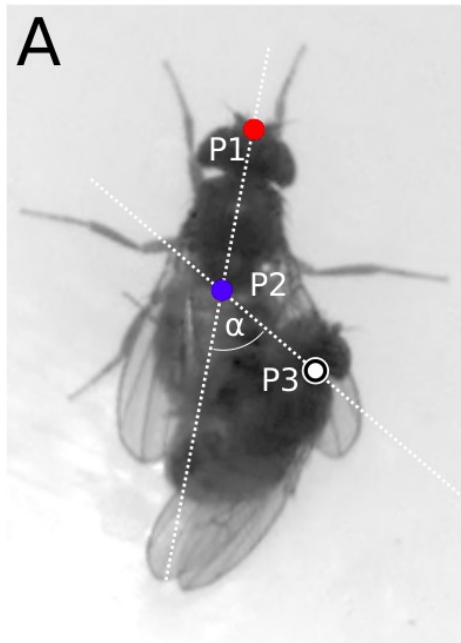


409 **Figure 1 supplement 3. Crossing scheme for time-lapse microscopy**  
 410 **samples.** Homozygous females [ $myoID^{mut/mut}$ ,  $act5C::DE-Cad-EYFP_2^{+/+}$ ] were  
 411 crossed to wild-type males [ $myoID^{wt/wt}$ ,  $act5C::DE-Cad-EYFP_2^{-/-}$ ]. The female F1  
 412 progeny was crossed back to wild-type males and male progeny was crossed to  
 413  $myoID$  homozygous mutant males [ $myoID^{mut/mut}$ ,  $act5C::DE-Cad-EYFP_2^{-/-}$ ]. The  
 414 progeny of the latter cross was then maintained by sibling crosses: females  
 415 [ $act5C::DE-Cad-EYFP_2^{+/-}$ ] with males [ $act5C::DE-Cad-EYFP_2^{-/-}$ ] and females  
 416 [ $act5C::DE-Cad-EYFP_2^{-/-}$ ] with males [ $act5C::DE-Cad-EYFP_2^{+/-}$ ]. The presence  
 417 of the  $act5C::DE-Cad-EYFP_2$  insertion was visible under a fluorescence  
 418 stereomicroscope by the presence of red fluorescence in the adult eyes. Colored  
 419 circles indicate  $myoID$  genotypes, green:  $myoID^{wt/wt}$ , yellow:  $myoID^{wt/mut}$ , red:  
 420  $myoID^{mut/mut}$ . Outlines indicate  $act5C::DE-Cad-EYFP_2$  insertion, absent: no  
 421 insertion, dashed: heterozygous insertion/no insertion, full: homozygous for the  
 422 insertion. Open squares indicates genotypes of individuals used for time-lapse  
 423 imaging. Times-lapse imaging was performed on individuals originating from the  
 424 first three successive generations.



425 **Figure 2 supplement 1. Mating behavior of *D. pachea* males differing in**  
 426 ***myoID* genotype.** This ethogram summarizes mating behavior observations  
 427 (Source datafile 4) of copulation recording trials (Source datafile 3). Each line  
 428 presents one mating trial and trials are grouped by male *myoID* genotype. Green  
 429 circles indicate courtship start, red segments indicate male licking behavior, blue  
 430 segments mounting attempts, grey segments stable copulation, overlaid by  
 431 black tick marks that indicate moments of mating position measurements (Source  
 432 datafile 5). In one trial copulation is labeled “ventral view” because the copulation  
 433 was observed in ventral view so that position landmarks (Figure 2 supplement 2)  
 434 could not be determined. The arrow on the right indicates the orientation of male  
 435 genitalia (Figure 1, Source datafile 1) with 0° on top. ND indicates non  
 436 determined genitalia orientation angles.

437



439 **Figure 2 supplement 2. Quantification of copulation postures. (A)**  
440 Landmarks to approximate the male head position relative to the female midline  
441 as described in (Acurio et al., 2019): P1 (red point) is the anterior medial tip of  
442 the female head, P2 (blue point) the distal tip of the female scutellum and P3  
443 (white open circle) is the most posterior medial point of the male head (Source  
444 datafile 5). The angle ( $\alpha$ ) between white lines (P1-P2) and (P2-P3) was used to  
445 measure sidedness of the mating position on each extracted image. **(B)** Scatter  
446 plot of mating angles obtained from two replicate analyses from two persons,  
447 Pearson correlation ( $t = 50.193$ ,  $df = 175$ ,  $p < 2.2 \times 10^{-16}$ ,  $r = 0.9669795$ ). The red  
448 dashed line corresponds to the linear regression line. Variation in angle estimates  
449 was found to be attributable mostly to individual images of the different movies  
450 (image) but not to replicate measurements (replicate) (ANOVA, angle ~ image +  
451 replicate, image:  $df1 = 176$ ,  $df2 = 1$ , image:  $F = 58.74$ ,  $p < 10^{-16}$ , replicate:  $F =$   
452  $0.148$ ,  $p = 0.701$ ). **(C-H)** landmark positions of each analysis and genotype,  
453 rotated and scaled relative to the distance P1-P2. All P2 points were super-  
454 imposed onto the diagram origin and P1 points were aligned onto position (0,1).  
455 The FM axis corresponds to the female midline, PFM axis is perpendicular to the  
456 female midline.

457 **Movie 1.** Clockwise genitalia rotation, acquired by time-lapse microscopy of a *D.*  
458 *pachea* heterozygous *myoID*<sup>wt/mut</sup> mutant male (Source datafile 1, individual 260).

459 **Movie 2.** Counter-clockwise genitalia rotation, acquired by time-lapse microscopy  
460 of a *D. pachea* homozygous *myoID*<sup>mut/mut</sup> mutant male (Source datafile 1,  
461 individual 274).

462 **Source datafile 1** Male *D. pachea* genitalia morphology and orientation,  
463 spreadsheet with length and orientation measurements of genital morphology of  
464 male *D. pachea* flies.

465 **Source datafile 2** Time-lapse microscopy trials, summary of trials and conditions  
466 for time-lapse microscopy.

467 **Source datafile 3** Single couple mating trials, summary of *D. pachea* single  
468

469  
470

471  
472